also assign a somewhat reduced polarizability of 1.0 for CIM+ and the equivalently mapped CGD+, the central carbon atoms in these cationic systems. Finally, for O+, O=+, and O%+, formally charged oxygens of hybridization sp^3, sp^2, and sp, respectively, we take 0.4 for the polarizability. To be sure, these polarizabilities cannot be said to be known accurately, but we include them in Table XIII to suggest how vdW parameters might be expected to behave in such chemical environments.

Continuous Symmetry Measures

Hagit Zabrodsky,[‡] Shmuel Peleg,[‡] and David Avnir*

Contribution from the Departments of Computer Science and Organic Chemistry, The Hebrew University of Jerusalem, 91904 Jerusalem, Israel. *Received November 25, 1991*

Abstract: We advance the notion that for many realistic issues involving symmetry in chemistry, it is more natural to analyze symmetry properties in terms of a continuous scale rather than in terms of "yes or no". Justification of that approach is dealt with in some detail using examples such as: symmetry distortions due to vibrations; changes in the "allowedness" of electronic transitions due to deviations from an ideal symmetry; continuous changes in environmental symmetry with reference to crystal and ligand field effects; non-ideal symmetry in concerted reactions; symmetry issues of polymers and large random objects. A versatile, simple tool is developed as a continuous symmetry measure. Its main property is the ability to quantify the distance of a given (distorted molecular) shape from any chosen element of symmetry. The generality of this symmetry measure allows one to compare the symmetry distance of several objects relative to a single symmetry element and to compare the symmetry distance of a single object relative to various symmetry elements. The continuous symmetry approach is presented in detail for the case of cyclic molecules, first in a practical way and then with a rigorous mathematical analysis. The versatility of the approah is then further demonstrated with alkane conformations, with a vibrating ABA water-like molecule, and with a three-dimensional analysis of the symmetry of a [2 + 2] reaction in which the double bonds are not ideally aligned.

1. Continuous Symmetry Measures. Why Are They Needed?

One of the most deeply-rooted paradigms of scientific thought is that Nature is governed in many of its manifestations by strict symmetry laws. The continuing justification of that paradigm lies within the very achievements in human knowledge it has created over the centuries.[1,2] Yet we argue that the treatment of natural phenomena in terms of "either/or", when it comes to a symmetry characteristic property, may become restrictive to the extent that some of the fine details of phenomenological observations and of their theoretical interpretation may be lost. Atkins writes in his widely-used text on physical chemistry: "Some objects are *more symmetrical* than others",[3] signaling that a scale, quantifying this most basic property, may be in order. The view we wish to defend in this report is that symmetry can be and, in many instances, should be treated as a continuous "gray" property, and not necessarily as a "black or white" property which exists or does not exist. Why is such a continuous symmetry measure important? In short, replacing a "yes or no" information processing filter, which acts as a threshold decision-making barrier which differentiates between two states, with a filter allowing a full range of "maybe's", enriches, in principle, the information content available for analysis.

This report contains four sections. In the next section we develop in some detail the notion of the need for a symmetry scale. It is an important part of the report because the very question at hand is not trivial and is certainly not standard or routine, and some readers may need persuasion that efforts to answer this question are worthwhile and may perhaps lead to a useful framework of discussion of symmetry issues in chemistry.[4-7] Yet, we recall at this point that the door to the questions we pose has been at least partially opened. For instance, Murray-Rust et al. have suggested the use of symmetry coordinates to describe nuclear configurations of MX_4 molecules that can be regarded as distorted versions of the T_d symmetrical reference structure.[8,9] More recently, Mezey and Maurani[10,11] extended the point symmetry concept for quasi-symmetric structures by using fuzzy-set theory (terming it "syntopy" and "symmorphy") and provided a detailed demonstration of its application for the case of the water molecule.[12] Also of relevance are proposals for chirality scales (for some different approaches, see, for example, refs 13 and 14).

In Section 3, we offer a tool for the quantitative assessment of symmetry contents which is, we believe, efficient, easy to implement, and general in the sense that it is applicable to a wide and diverse array of symmetry problems as detailed below. All the required principles and practical aspects of this tool are given in Section 3 using cyclic structures as examples. For the interested reader and for sake of completeness, we provide rigorous mathematical proofs in the Appendix. In Section 4 we demonstrate the implementation of our approach on three additional problems: conformations of open-chain *n*-alkanes, the vibrating water-like molecule, and the symmetry of a [2 + 2] concerted reaction. These three examples are but the tip of the iceberg, the outlines of which

[‡] Department of Computer Science.
* Department of Organic Chemistry.

(1) *Symmetry: Unifying Human Understanding*; Hargittai, I., Ed.; Pergamon Press: New York, 1986. *Symmetry 2: Unifying Human Understanding*; Hargittai, I., Ed.; Pergamon Press: Oxford, 1989.
(2) *Symmetries in Science. III*; Gruber, B., Iachello, I., Eds.; Plenum Press: New York, 1988 and earlier volumes in that series.
(3) Atkins, P. W. *Physical Chemistry*, 3rd ed.; Oxford University Press: Oxford, 1986, p 406.
(4) Hargittai, I.; Hargittai, M. *Symmetry Through the Eyes of a Chemist*; VCH: Weinheim, 1986.
(5) Ezra, G. S. *Symmetry Properties of Molecules*; Springer: Berlin, 1982.
(6) For an excellent collection of classical papers, see: *Symmetry in Chemical Theory*; Fackler, J. P., Jr., Ed.; Dowden, Hutchison & Ross: Stroudsburg, PA, 1973.
(7) Mezey, P. G. *J. Am. Chem. Soc.* **1990**, *112*, 3791.
(8) Murray-Rust, P.; Bürgi, H. B.; Dunitz, J. D. *Acta Cryst.* **1978**, *B34*, 1787.
(9) Luef, W.; Keese, R.; Bürgi, H. B. *Helv. Chim. Acta* **1987**, *70*, 534.
(10) Maruani, J.; Mezey, P. G. *C. R. Hebd. Séances Acad. Sci. Paris*, II, **1987**, *305*, 1051 (Erratum: *Ibid.* **1988**, *306*, 1141). Mezey, P. G.; Maruani, *J. Mol. Phys.* **1990**, *69*, 97.
(11) Mezey, P. G. In *New Theoretical Concepts for Understanding Organic Reactions*; Bertrán, J., Csizmadia, I. G., Eds.; Kluwer: Dordrecht, 1989; pp 55, 77.
(12) The problem of symmetry fuzziness is also described in the Introduction of ref 4 (pp 3–4).
(13) Gilat, G. *J. Phys. A* **1989**, *22*, L545.
(14) Hel-Or, Y.; Peleg, S.; Avnir, D. *Langmuir* **1990**, *6*, 1691.

0002-7863/92/1514-7843$03.00/0 © 1992 American Chemical Society

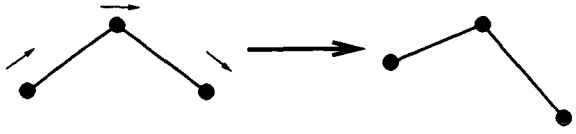

Figure 1. The distortion of the C_{2v} symmetry of a water molecule by the ν_3 vibration mode.

are given next.

2. Continuous Symmetry Measures. Where Are They Needed?

Everywhere, we believe. Here is a selection of specific examples which illustrate our main argument.

2.1. "Allowed" and "Forbidden" Transitions in Electronic Spectra. The present report was seeded in an earlier study.[15] There, Meyer suggested the following. Consider, for instance, the very weak ($\epsilon_{max} \approx 200$) forbidden $\pi \rightarrow \pi^*$ transition to the lowest-lying singlet in benzene ($A_g^1 \rightarrow B_{2u}^1$) and compare it with the carbon skeleton of toluene. The D_{6h} symmetry of the benzene hexagon changes to a distinctly different point group, C_{2v}, yet the extinction coefficient increases only to $\epsilon_{max} = 225$. Current wisdom of accounting for the discrepancy between the major symmetry change and the small effect in the "allowedness" of the transition is to use such arguments that "the methyl perturbs the π system only to a small extent"; i.e., the day is saved by resorting to "local" symmetry. We suggest that a natural way to present this problem is to ask: By how much does the symmetry of toluene deviate from D_{6h}? That this type of question is indeed more natural for approaching electronic transitions is further evident by taking the above example to an extreme, i.e., comparing the benzene/deuterobenzene pair. Again, the situation is of D_{6h} versus C_{2v}, yet physical intuition suggests that, when properties of these two molecules are comparatively analyzed, it is more reasonable to determine the ΔD_{6h} of the latter than ascribe C_{2v} to it. For an account of the successes of perturbation approaches such as "near symmetry groups", see for example, ref 16.

2.2. Vibrations and Dynamic Properties of Molecules.[17] Some of the properties of molecules can be discussed in terms of their "frozen" structure, which is usually taken to be the equilibrium stable structure. However, many other properties are directly linked to the more realistic picture of an ever-dynamic molecule, which vibrates, rotates, and translates. The symmetry problematics described above appear here too. Consider, for instance, the vibrating water molecule. This is a C_{2v} molecule and its ν_1 and ν_2 vibrational modes preserve this symmetry. But what about ν_3? This vibrational mode distorts the C_{2v} symmetry (Figure 1), and, again, a legitimate question is by how much does the molecule deviate from C_{2v} after 1% of one cycle, after 10% of it, and so forth; ΔC_{2v} oscillates in time, and that oscillation is linked to a plethora of associated physical properties. One example is the changes in time of the dipole moment of the molecule due to that ν_3 mode and the consequent change in time of the probability of interaction with an external field. Indeed, coming back to electronic transitions, since vibrations can destroy a molecular symmetry to such an extent that a forbidden transition in an idealized perfect symmetry becomes partially allowed, one can, in principle, follow by our suggested approach the gradual relaxation of forbiddenness along the time coordinate of a given vibrational mode.[18]

2.3. Crystal Field and Ligand Field Effects in Environments of Distorted Symmetry. A well-known phenomenon is the removal of the degeneracy of energy levels of a chemical species whenever contained in an environment of symmetry other than its own (a certain arrangement of ligands or a certain packing in the crystal). The degree of removal of degeneracy is directly linked to the "decrease" in the symmetry of the environment, compared to the isolated chemical species. Traditionally, this problem is treated in terms of jumps in the symmetry point group. For instance, the splitting of the degenerate p-orbitals increases from $a_{2u} + e_u$ in a D_{4h} environment to $a_1 + b_1 + b_2$ in a C_{2v} environment.[19] (Cf. also the celebrated Jahn–Teller effect which is based on symmetry destruction in molecules with partially filled orbitals.)

The recognition that environments exhibiting a continuous range of *distorted* symmetries are as abundant, if not more, than ideally symmetric environments, has spread fast, especially in the past decade.[20] For instance, ions, molecules, and ion–ligand complexes adsorbed on materials, such as metal oxides or encapsulated in inorganic glasses, experience not *one* environmental symmetry but *some* "symmetry ± Δsymmetry" (say, an octahedral liganding of a cation in an environment of amorphous (SiO_2)–O^- materials).[21] Again, it seems to us more natural to approach such systems in terms of a continuous symmetry scale.

2.4. Symmetry Rules for Reaction Coordinates and Orbital Symmetry Conservation. The principle of conservation of orbital symmetry has caused a quantum leap in the understanding of reaction pathways in organic chemistry. This is already well documented in elementary textbooks, which is a sign of its coming of age. The time therefore is ripe, it seems to us, to introduce some fine-tuning of the strict picture, and in particular to relax, again, the ideal "yes or no" situation to the real-world gray area which has been treated so far with difficulties and with ad hoc explanations. This is a vast field indeed, but it suffices to take one very basic problem to illustrate our point. Consider two ethylenes approaching each other for a [2 + 2] reaction. The answer to the question of whether that reaction is allowed thermally or photochemically, or whether a suprafacial or antarafacial process will take place, or whether the reaction will take place at all, is very much dependent on the symmetry of alignment of the two reacting molecules or moieties. The extremes are D_{2h} for a parallel approach and C_2 for an orthogonal approach, and it is predicted successfully[22] that the former is needed for a suprafacial photochemical formation of cyclobutane. Most of the time, however, the two ethylenes are *not* in an ideal D_{2h} arrangement. This may be due to an intramolecular frozen conformation of the two double bonds, to nonsymmetric sterical hindrance caused by substituents on the double bond, and to the dynamical nature of the system (rotations and translations especially in viscous media). We seek a tool that will enable one to answer the following basic question: What is the (static or dynamic) relation between the degree of deviation from a given symmetry and the allowedness of a reaction? In our case: what is the relation between changes in ΔD_{2h} or C_2 and, e.g., the reaction rate of a photochemical [2 + 2] reaction?

2.5. Ordering in Molecular Assemblies. The efficiency with which assemblies of molecules pack or undergo phase transition is very much determined by their (static) shape symmetry. This is true for crystallization, for packing of monolayers, for ordering within the shells of micelles, for ordering within domains of liquid crystals, within Langmuir–Blodget films, within islands of adsorbates in submonolayer coverages and within the complete monolayer. A continuous symmetry measure may help quantify the relation between molecular shape and ordering in all of these assemblies. Motivated by this packing problem, Kitaigorodskii suggested in his classical work[23] to use non-overlapping volumes of two enantiomers as a suitable measure.

2.6. Symmetry of Polymers and of Large Random Objects. Much effort has been invested in recent years in understanding the mechanism of formation, the chemical properties, and the

(15) Avnir, D.; Meyer, A. Y. *J. Mol. Struct. (THEOCHEM)* **1991**, *226*, 211.

(16) Bunker, P. R. *Molecular Symmetry and Spectroscopy*; Academic Press: New York, 1979, Chapter 11.

(17) Cf.: (a) Longuet-Higgins, H. C. *Mol. Phys.* **1963**, *6*, 445. (b) Chapter 3 in ref 5.

(18) Distorted hexagons are used intensively in Section 3. For a pioneering study of the vibrational distortions of a hexagon, see: Wilson, E. B. *Phys. Rev.* **1934**, *5*, 706.

(19) Tables 6-12 in ref 4.

(20) *On Growth and Form*; Stanley, H. E., Ostrowsky, N., Eds.; Martinus Nijhoff: Dordrecht, 1986.

(21) Levy, D.; Reisfeld, R.; Avnir, D. *Chem. Phys. Lett.* **1984**, *109*, 593.

(22) Fleming, I. *Frontier Orbitals and Organic Chemical Reactions*; Wiley: Chichester, 1987.

(23) Kitaigorodskii, A. I. *Organic Chemical Crystallography*; Consultants Bureau: New York, 1961; Chapter 4.

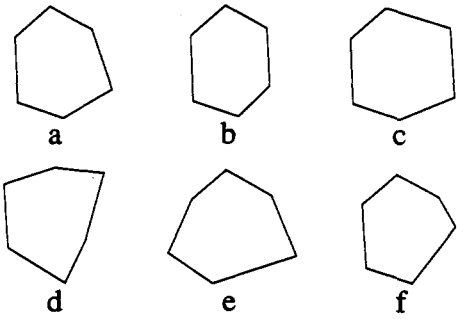

Figure 2. Distorted hexagons. By how much is each of these shapes distant from C_6 symmetry?

physical properties of disordered systems.[20,24] These include polymers, aggregates, clusters, electrodeposits, chemically sputtered surfaces, partially dissolved and reacted objects, precipitates, and powdered, crushed, and fractured objects. Many of the classical question marks which linked molecular level properties to their symmetry are applicable for the large, disordered, or imperfect objects as well. For instance, one can ask by how much does the C_6 symmetry of a growing snowflake fluctuate around the ideal C_6 structure along the time axis of its growth? Or one can ask: given a random growth process such as an electrochemical deposition, what is the symmetry of that electrodeposited aggregate?[25] And even more interesting, repeating such an experiment twice, do the two products have the same symmetry despite being randomly non-identical? And how do properties like, e.g., impedance differ between these two objects as a consequence of a slight variation in symmetry? By virtue of the random element in a growth process, all objects formed by it are distinctly different from each other, for instance, in the sense that they are not superimposable; yet they "look alike" and one can easily recognize that they belong to the same "species". Such situations call for a major change in the description of a geometrical object; one is better off replacing specific, point by point descriptions, with global descriptors. What then is a suitable global continuous symmetry descriptor of large random objects? What are the implications of discussing the symmetry properties of objects that can never be formed again?

These are but some of a much longer list of classical problems in chemistry which are intimately associated with issues of symmetry,[3-7] and which, we believe, may gain from the refinement of the "yes or no" attitude. Having explained the rationale of this need, we make a specific and explicit suggestion of how to approach it in the next section.

3. Continuous Symmetry Measures (CSM): The Method

3.1. General Properties of the CSM and Its Definition. Figure 2 shows distorted hexagons, perhaps some frozen moments in the distortional vibration of benzene. We seek to answer the following question. By how much is each of these objects distant from a rotational C_6 symmetry, or from a C_3 symmetry, or from a C_2 symmetry (actually regular hexagons are D_{6h}, but we concentrate here on only one of its symmetry elements), or from a reflection σ symmetry? We emphasize that we are dealing with deviation from a symmetry element and *not* with a deviation from a specific object having the required symmetry. Thus, although it is a straightforward guess that the C_6 object in the above example is an ideal hexagon, it is not known a priori what is the exact shape of the C_3 object which is closest to each of the distorted hexagons. Our method identifies that the minimal correctional procedure on the hexagon in Figure 2f toward an ideal C_3 object yields object c in Figure 3. In fact, our method provides a *set* of distances to various symmetry elements (Figure 3) and identifies which is the closest. Additionally, we obtain the explicit shapes which correspond to each of these closest symmetries (Figure 3).

(24) *Scaling Phenomena in Disordered Systems*; Pynn, R., Skjeltorp, A., Eds.; Plenum: New York, 1985.
(25) Pajkossy, T. *J. Electroanal. Chem.* **1991**, *300*, 1.

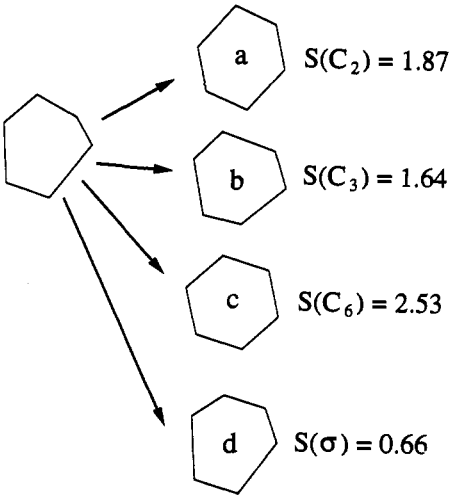

Figure 3. The C_2, C_3, C_6 and σ symmetry shapes closest to the distorted hexagon of Figure 2f. Corresponding symmetry values (defined below) are displayed. It is seen, for example, that the distorted hexagon is "much more" σ-symmetric than C_6-symmetric.

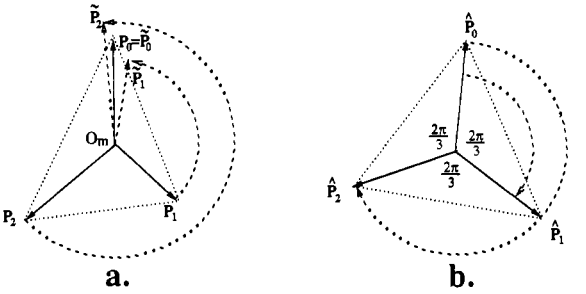

Figure 4. The continuous symmetry measure procedure for evaluating the C_3 symmetry of a triangle P_0, P_1, P_2. Follow Section 3.2 with this figure.

Definition: The continuous symmetry measure quantifies the minimal distance movement that the points of an object have to undergo in order to be transformed into a shape of the desired symmetry. In practice, the sum of the squares of these distances is taken (being isotropic, continuous, and differentiable; see Appendix), normalized to the size of the object. We refer to this operation as the **symmetry transformation** (ST).

In this report we restrict ourselves to the *shape* of molecules, and not to their mass or electronic distributions. Relaxing this limitation will require a selection of molecular properties other than shape, e.g., charge distribution contours, but will not require principal changes in the method. We treat here the basic symmetry operations of rotation and reflection; combinations thereof, i.e., symmetry groups, are left for subsequent reports.

3.2. Deviation of Imperfect n-Gons from C_n Symmetry. We explain and discuss most of the properties of the ST for the case of polygons in two dimensions and extend it to additional cases, including a three-dimensional case in Section 4. We begin with the basic question: by how much does a distorted polygon of n vertices deviate from a C_n symmetry? For the sake of simplicity, let us take the case of the smallest n, a triangle (*any* triangle), and ask by how much is it distant from a C_3 symmetry? The procedure employed to answer it is as follows (Figure 4).

Given a polygon (triangle) whose vertices are P_0, P_1, P_2 in a clockwise order (Figure 4a):

1. Identify the center of mass of the shape (in our case, the triangle), O_m. This is done by averaging the x,y coordinates of the vertices.

2. Scale the size of the object so that the longest distance from O_m to any one of the vertices is one.

3. Fold points P_i as follows: rotate vertex P_i counterclockwise around O_m by $2\pi i/3$ radians. In our case rotation P_1 counterclockwise around O_m by $2\pi/3$ radians and P_2 by $4\pi/3$ radians

Table I. Continuous Symmetry Measure S Values of Various Distorted Hexagons

shape[a]	$S(C_2)$	$S(C_3)$	$S(C_6)$	$S(\sigma)$
a	0.46	0.88	1.26	0.18
b	0.12	1.61	1.63	0.23
c	0.61	0.78	1.00	0.27
d	1.80	1.38	2.96	1.53
e	2.41	1.59	2.63	1.70
f	1.87	1.64	2.53	0.66

[a] See Figure 2.

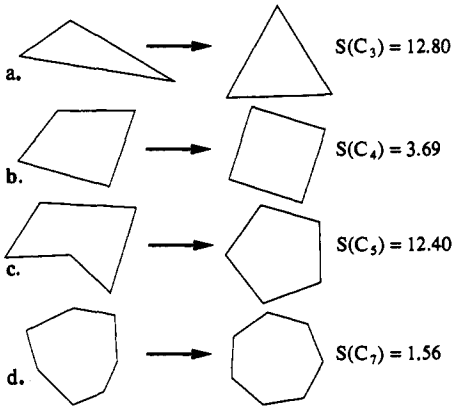

Figure 5. The distance of various n-gons to their corresponding C_n symmetries and the closest C_n-symmetric shapes.

(Figure 4a). P_i is converted to $\tilde{P}_i$, i.e., P_0, P_1, P_2 are converted to $\tilde{P}_0$, $\tilde{P}_1$, $\tilde{P}_2$ (where $\tilde{P}_0 = P_0$).

4. Average the three vectors $\tilde{P}_0$, $\tilde{P}_1$, $\tilde{P}_2$ obtaining $\hat{P}_0$.

5. Unfold $\hat{P}_0$ as follows (Figure 4b): rotate $\hat{P}_0$ clockwise around O_m by $2\pi i/3$ radians, obtaining $\hat{P}_i$. In our case: $\hat{P}_0$ remains in place; $\hat{P}_1$ is obtained by rotating $\hat{P}_0$ $2\pi/3$ radians clockwise and $\hat{P}_2$ by $4\pi/3$. A C_3-symmetric triangle is obtained.

6. The averaged square of the translation distances P_0 to $\hat{P}_0$, P_1 to $\hat{P}_1$, and P_2 to $\hat{P}_2$ is the symmetry measure of the original triangle, with respect to C_3.

In general, we define the *C_n-folding* of n points, as the rotation of each P_i around the center of mass by $2\pi i/n$ radians counterclockwise forming $\tilde{P}_i$. These are then averaged to obtain $\hat{P}_0$ which is *C_n-unfolded* by clockwise rotation around the same center by $2\pi i/n$ radians obtaining $\hat{P}_i$. The original set of points is thus transformed into a set which has a C_n symmetry. The continuous symmetry measure, S, of the original points is the averaged square of the transitions P_i to $\hat{P}_i$:

$$S(\text{sym}) = 100\frac{\sum_{i=0}^{n-1}\|P_i' - \hat{P}_i\|^2}{n}$$

where (sym) indicates the symmetry element under study and the factor of 100 is introduced only for convenience of handling the S values. In the Appendix we prove that S is a minimal distance value. S can take values between 0 and 100. $S(\text{sym}) = 0$ means that the object has the undistorted symmetry. The maximal value for S is obtained when the "closest" symmetrical shape is a point (see Appendix, section B).

Returning to Figure 2 we can now provide the $S(C_6)$ values of the various distorted hexagons; these are given in Table I. And in Figure 5 a number of different n-gons along with their $S(C_n)$ values are given. The two figures serve not only for demonstrating the method, but also to help develop an intuitive feeling of the relation between the S values and the actual deviations from the symmetry elements.

3.3. Deviation of an Imperfect n-Gon from C_m ($m < n$). For distorted n-gons one can also ask: what is its deviation from a C_m symmetry which is lower than C_n? For instance, on each of the hexagons of Figure 2, one can ask that question for C_2 and C_3. In general, it is more natural to ask that question for C_m with $n = qm$ where q is an integer. (Thus, assessing by how much is a distorted hexagon distant from C_4, C_5 is left for the moment although it is possible to carry out this calculation as well.) The evaluation of $S(C_m)$ is demonstrated for a hexagon and is performed as follows.

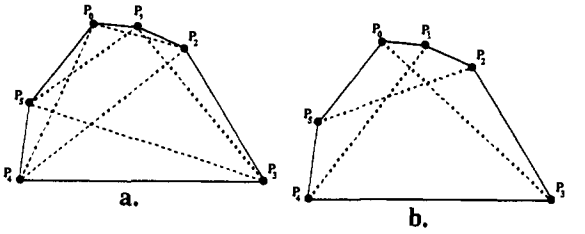

Figure 6. The division of the vertices of an n-gon into subsets for the calculation of $S(C_m)$ values (where $m < n$): (a) two triangles for calculating $S(C_3)$, (b) three diagonals for calculating $S(C_2)$. Follow Section 3.3, step 1, with this figure.

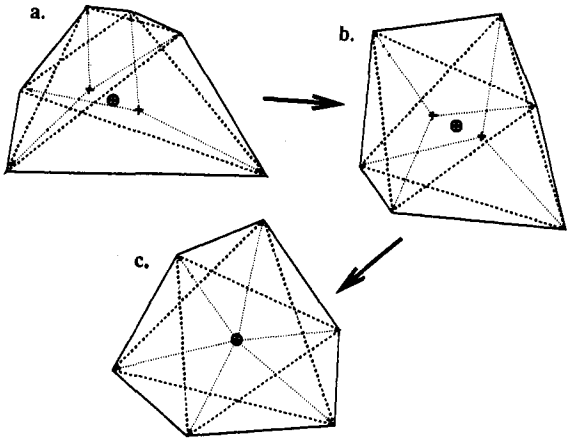

Figure 7. Obtaining the symmetry value and a C_3-symmetric hexagon from the distorted hexagon of Figure 6. a→b is performed as in Figure 4. b→c is performed by translating each subset of vertices such that its center of mass (+) coincides with the center of mass of the object (⊕). Follow Section 3.3, steps 2 and 3, with this figure.

1. In order to obtain a C_m ($n = qm$) symmetry for an n-polygon, one first divides the set of all n vertices to q subsets of m vertices each (Figure 6). These subsets are selected to connect m vertices so that they are separated from each other by $(n/m) - 1$ vertices. In a hexagon this means two triangles for $m = 3$ (Figure 6a) and three diagonals for $m = 2$ (Figure 6b).

2. Each of the m-gons is symmetrized to C_m as described in the previous section for Figure 4a. In our case, two triangles are symmetrized to C_3 (Figure 7a → Figure 7b).

3. Each of the symmetrized m-gons (or diagonal) is translated minimally to coincide its shape center of mass with the center of the original n-gon (Figure 7b → Figure 7c). The resulting object is an n-gon with a C_m symmetry (in our case, a C_3 hexagon).

4. The S value is calculated as in step 6 above.

The proof that this procedure is the minimal most efficient operation is given in the Appendix. Table I collects the CSM values of $S(C_2)$, $S(C_3)$, and $S(C_6)$ for the set of hexagons shown in Figure 2.

3.4. Reflection Symmetry. Reflection is the second basic symmetry operation we treat here. A CMS for this case is constructed in a similar way to the rotational symmetry measure as follows (Figure 8). Given a pair of points P_0, P_1 and a reflection axis (O_m, θ):

1. Denote $P_0 = \tilde{P}_0$.

2. Reflect P_1 across the reflection axis obtaining $\tilde{P}_1$ (Figure 8a).

3. Average the vectors $\tilde{P}_0$ and $\tilde{P}_1$ obtaining $\hat{P}_0$.

4. Reflect back $\hat{P}_0$ across the reflection axis obtaining $\hat{P}_1$ (Figure 8b).

5. The CSM $S(\sigma)$ value of the original pairs of points is obtained by averaging the squared distances P_0 to $\hat{P}_0$ and P_1 to $\hat{P}_1$.

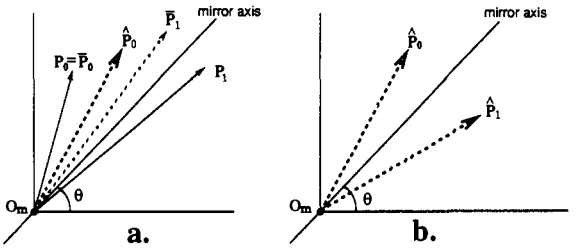

Figure 8. Calculating the $S(\sigma)$ value of a pair of points P_0, P_1 given a reflection axis (O_m, θ). (a) Reflect P_1 across the reflection axis obtaining $\{\bar{P}_0, \bar{P}_1\}$ and average them obtaining $\hat{P}_0$. (b) Reflect $\hat{P}_0$ across the reflection axis obtaining $\hat{P}_1$. $\hat{P}_0$ and $\hat{P}_1$ are σ-symmetric. Follow Section 3.4 with this figure.

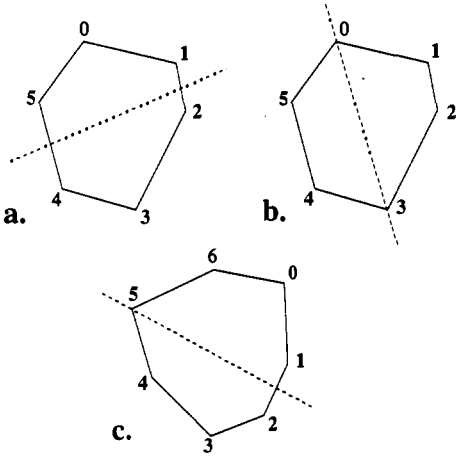

Figure 9. Pairing vertices for evaluation of $S(\sigma)$ values (see Section 3.4).

To evaluate the reflection symmetry in a polygon of m vertices, we divide its vertices into pairs and then perform the above procedure for every pair. Pairing vertices of a polygon is performed by dividing its sequence of vertices into two subsequences of equal length while preserving their ordering. Reflection symmetric pairing is performed between vertices of the two subsequences. Thus a possible division of the vertices of the hexagon in Figure 9a is {2,3,4} and {5,0,1} with the corresponding pairing {2,1}, {3,0}, and {4,5}. If the given polygon has an odd number of vertices, one of the vertices is duplicated, and the division of the sequence of vertices is such that each subsequence includes a copy of the vertex. Thus the heptagon in Figure 9c can be paired as: {5,5}, {4,6}, {3,0}, and {2,1}. If the given polygon has an even number of vertices, a pairing may be performed by duplicating two vertices which are $m/2$ vertices apart. Thus the hexagon in Figure 9b can also be paired: {0,0}, {5,1}, {2,4}, and {3,3}.

In general, to evaluate the CSM for reflection symmetry of a given polygon, perform the following.

1. Pair the vertices of the polygon.
2. Normalize the shape (as in steps 1 and 2 in Section 3.2).
3. Evaluate $S(\sigma)$ of each pair over a given symmetry axis, as previously described.
4. Average the $S(\sigma)$ values of all the pairs obtaining the $S(\sigma)$ value of the polygon.
5. Minimize the $S(\sigma)$ value over all possible pairings of the vertices.

If a reflection axis is not chosen a priori, then minimization over all possible reflections axis is performed. (In the Appendix we show that this minimization has an analytical solution.) Figure 10 shows a number of shapes, their $S(\sigma)$ values, and the symmetrized objects obtained. See also Table I for the $S(\sigma)$ of the hexagons of Figure 2.

In the next section we provide some additional examples of how the CSM procedure is applied.

4. Continuous Symmetry Measures: Further Examples

4.1. Linear and Branched Distorted π-Systems. Having concentrated on polygons in Section 3, we first show how to extend the method to polylines. The conformational freedom of polylines, e.g., n-alkenes (or n-alkanes), is of course much richer than polygons, ranging from all-trans to all-cis and anywhere in between. In such cases, it is helpful (though not necessary) if one confines oneself to the symmetry analysis of the conformer of interest. For instance, if one wishes to analyze the symmetry constrains on the Cope rearrangement of 1,3,5-hexatriene, then the all-cis conformer is of relevance. The treatment of these cases is along the same procedural lines employed for the polygons: P_0 and P_5 are closed with an imaginary line and symmetrization is carried out as in Section 3. Examples are the hexagons of Figure 2 in which one bond is opened, with the corresponding S values in Table I. The strength of our approach is, however, that it is not necessary to "guess" what is the suitable conformer of hexatriene. It is capable of finding that the closest suitable conformer of the distorted all trans is the perfect all-cis. This is shown in Figure 11.

The approach to branched molecular skeletons is similar. For instance, if the $S(C_2)$ value of a tetrasubstituted ethylene is sought, then, as in the case of the hexagon, the three subset pairs are P_1–P_1', P_2–P_2', and P_3–P_3' (Figure 12).

4.2. The Vibrating ABA Molecule. In Figure 1 we showed a snapshot of the third vibrational mode of a water-like ABA molecule which reveals a distortion from C_2 symmetry. We are ready now to present it quantitatively: In Figure 13 (line a) the $S(C_2)$ spectrum for a full cycle is shown. The symmetry axis is not in a fixed location (see Figure 14b) although it always passes through B (the oxygen, in the case of water) and is chosen so as to give the minimal S value. It is seen that the CSM behavior of this system shows two maxima and two minima in one cycle. This is a reflection of the left–right symmetry within one cycle; except for the minima, molecular shapes separated by half a cycle

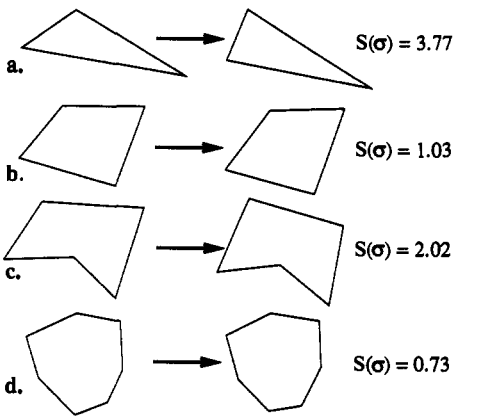

Figure 10. The $S(\sigma)$ values of various n-gons and their closest σ-symmetric shapes.

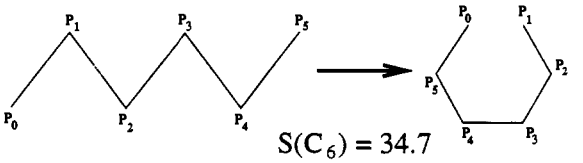

Figure 11. The distance of a distorted all-trans hexane skeleton to an all-cis. The CSM method identifies that the closest suitable conformer of the all-trans is the all-cis.

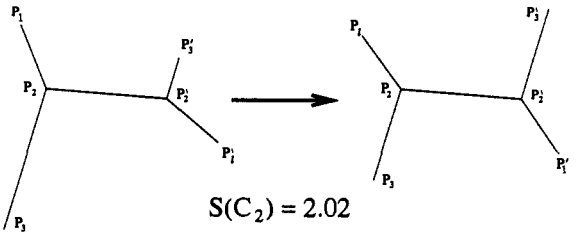

Figure 12. The $S(C_2)$ value and the closest C_2-symmetric shape of a distorted substituted ethylene.

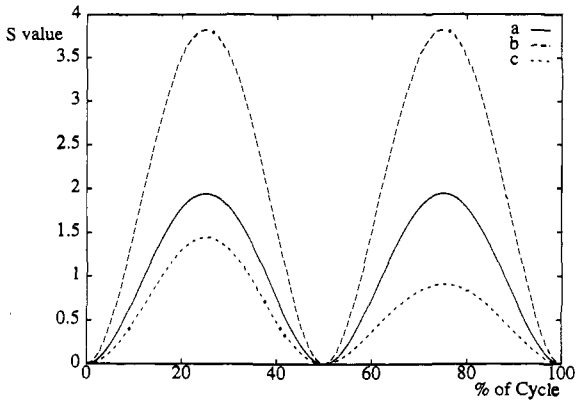

Figure 13. The changes in $S(C_2)$ during one cycle of a vibrating water-like hypothetical ABA molecule: (a) the ν_3 vibration mode. Both A's and B oscillate harmonically. The maximal stretching of A–B and maximal movement of B is 25% of the A–B bond length at the perfectly C_2-symmetric state. (b) As in (a) but B is fixed. (c) As in (a) but B and one of the A's are fixed.

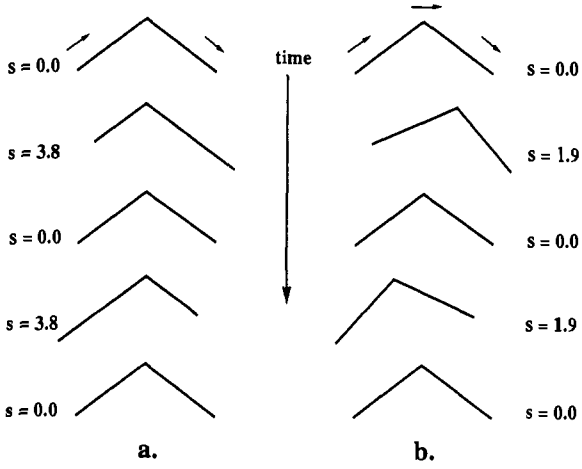

Figure 14. The molecular positioning of the vibrating ABA molecule at (a) the four extremum points of line b of Figure 13; (b) the four extremum points of line a of Figure 13.

are enantiomeric pairs in two dimensions. Thus, the CSM scale serves here also as a continuous chirality measure;[13,14] the shapes at the maxima are much more chiral than shapes that just emerge from the minima. Our tool additionally enables the isolation of the effects of specific atomic motions in a complex vibrational mode. For instance, line b in Figure 13 shows what happens if the vertex B is frozen in the ν_3 mode under analysis here. The S values almost double; that is, we see that the small left–right movements of B has a correctional effect on the distortive effect of the A–B stretchings. This effect is clearly seen in Figure 14. Incidentally, such freezing of one atom is not entirely hypothetical. Imagine, for instance, B being a surface moiety and the two A's as dangling surface-derivatizing residues. One can go on with this, and let only one A–B bond vibrate (the result is also shown in Figure 13, line c; the symmetry of the two half-cycles is eliminated as expected).

4.3. The [2 + 2] Concerted Reaction. A Three-Dimensional CSM Analysis. We are now ready to present the problem of non-ideal alignment symmetry for a concerted reaction, in a quantitative way. The specific case used in Section 2 (example 4) for illustrating that problem was of a [2 + 2] concerted reaction. The rate of this reaction, as well as any other concerted reaction, should be greatly determined by the degree at which the symmetry of the system deviates from the ideal. Following is the CSM approach to quantify this deviation (Figure 15).

Two ethylenes, P_1, P_3 and P_0, P_2, are placed in the xz plane as shown (the p-orbitals, not shown, are properly aligned in that plane). Deviation from this ideal D_{2h} arrangement can be expressed in terms of three rotations of P_1, P_3, leaving P_0, P_2 fixed:

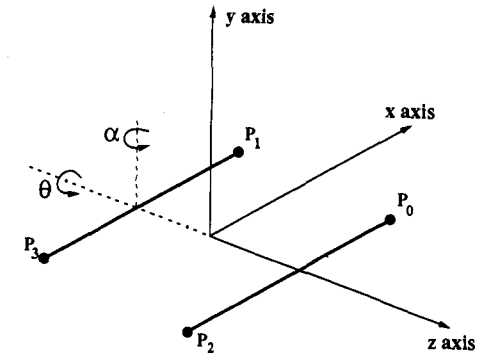

Figure 15. The ideal alignment of two reacting ethylenes (P_1,P_3 and P_0,P_2), and the angles of rotation (α, θ) which cause deviation from that symmetry.

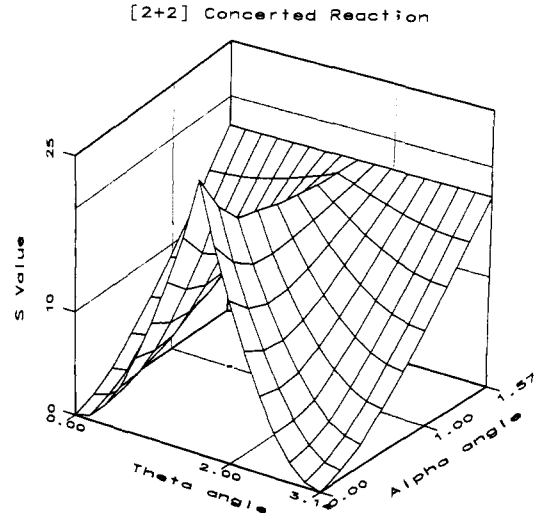

Figure 16. The CSM behavior of the mutual alignment of two ethylenes. θ and α are defined in Figure 15.

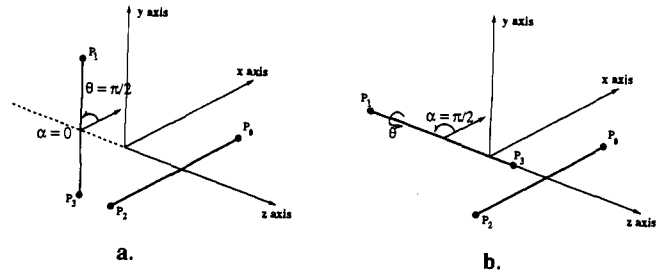

Figure 17. Two extreme non-ideal alignments of the ethylenes of Figure 15. In Figure 16 these are: (a) the forefront maximum tip and (b) the back straight line.

rotation around the z axis with an angle θ; rotation around an axis parallel to the y axis, as shown, with an angle α; and rotation around the P_1–P_3 axis. For sake of clarity, we omit the third rotation (though it can easily be added if desired). We thus reduce the problem to the following: what is the CSM behavior of two segments in space with reference to an ideal parallel alignment? Evaluation of $S(D_{2h})$ requires the calculation of $S(\sigma_{xy},\sigma_{yz},\sigma_{xz})$, but in our case σ_{xz} is redundant and, therefore, in practice, we measure $S(\sigma_{xy},\sigma_{yz})$. CSM calculations in 3D are not different in principle from the 2D $S(\sigma)$ calculations (Section 3.4), and some technical aspects of it are summarized in Part C of the Appendix. An important feature of the calculation is the following. We do not seek the deviation from a *specific* parallel alignment in a fixed xyz-frame of reference; for a reacting system the relevant value is the deviation from the *nearest* parallelism, and that can be at any set of angles in the fixed framework. The interesting three-dimensional map of results is shown in Figure 16. To

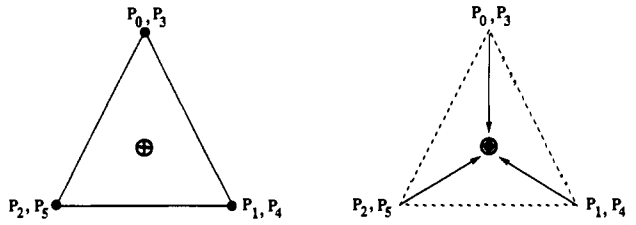

Figure 18. Demonstration of the extreme case, $S = 100$. Here it is the value of $S(C_2)$ for a hexagon which has pairs of vertices infinitely close to each other (a). The object closest to the hexagon, having C_2 symmetry is a point at the center of mass (b) (see part B of the Appendix).

explain it, let us start with the $\alpha = 0$ line, along which only θ changes. It is seen how the rotation around the z axis causes a gradual increase in the S value, reaching a maximum value at $\pi/2$ radians. Here the two ethylenes are perpendicular in two different planes (Figure 17a), the most distortive situation compared to D_{2h} parallelism. Let us now move to the other extreme, $\alpha = \pi/2$, which is shown in Figure 16 as a line parallel to the θ axis. Here the two ethylenes are perpendicular but in the *same* plane (Figure 17b), and θ rotation has no effect. It is also seen that perpendicularity in different planes ($\theta = \pi/2$; $\alpha = 0$) is less favorable than perpendicularity in the same plane ($\alpha = \pi/2$; any θ), and intuition agrees with that observation. The general trend for other θ, α combinations is more complex; α-tilting diminishes the distortive effect of θ-tilting except for a narrow window centered at $\theta = \pi/2$, where θ governs.

The approach, demonstrated here for the two ethylenes is general and can be applied to any other reactive system where the symmetry of the mutual alignment of the reactants, whether inter- or intramolecular, is crucial. We believe that the road is clear now for linking continuous symmetry changes to other reaction observables.

5. Conclusion

In this introductory paper we have concentrated on three aspects of continuous symmetry measures. First, we presented a detailed discussion on why such measures are needed in chemistry and in the natural sciences at large; second, we designed a general, easily implementable tool capable of measuring the symmetry content with regard to rotation and reflection; third, we gave a preliminary demonstration of its applicability in analyzing the symmetry properties of common cyclic and open structures, of a vibrating structure, and of interacting molecules. In subsequent reports we concentrate on the continuous symmetry properties of other symmetries, on symmetry issues of large random objects, and on correlating the CSM to other physical and chemical measurables as outlined in Section 2.

Acknowledgment. We thank S. Shaik and I. Hargittai for useful discussions and comments.

Appendix

A. The Symmetry Transform in 2D: Computations. A.1. C_n Symmetry. Given a set of vectors (whose source is the origin, and destinations are points of an object) $P_0, ..., P_{m-1}$, we assume $m = nq$. For simplicity we assume that the division into q subgroups of n vertices (as described in Section 3.3) is such that every n consecutive vectors constitute a subgroup (i.e., $\{P_{in}, ..., P_{in+(n-1)}\}$ for $i = 0...q-1$ is a subgroup). We wish to find the C_n-symmetry transformation of these vectors.

Denote by $N_0, ..., N_{m-1}$ the vectors obtained from $P_0, ..., P_{m-1}$ under the symmetry transformation. Following the symmetry transformation definition, the following must be minimized over $N_0, ..., N_{m-1}$:

$$\|N_0 - P_0\|^2 + ... + \|N_{m-1} - P_{m-1}\|^2$$

Denote by ω the center of mass of the transformed vectors. Since $N_0, ..., N_{m-1}$ constitute a C_n-symmetrical shape, the following must be satisfied:

$$N_1 = R_\theta(N_0 - \omega) + \omega$$
$$\vdots$$
$$N_{n-1} = R_\theta^{n-1}(N_0 - \omega) + \omega$$

where R_θ is the matrix of rotation by angle $2\pi/n$.

In general, for each subgroup we have:

$$N_{in+1} = R_\theta(N_{in} - \omega) + \omega$$
$$\vdots$$
$$N_{in+(n-1)} = R_\theta^{n-1}(N_{in} - \omega) + \omega$$

(i.e., for each subgroup, the transformed vectors constitute a regular n-gon with center of mass coinciding with the center of mass of all transformed points).

Thus the following must now be minimized:

$$\|N_0 - P_0\|^2 + ... + \|R_\theta^{n-1}(N_0 - \omega) + \omega - P_{n-1}\|^2 + ... + \|N_{m-n} - P_{m-n}\|^2 + ... + \|R_\theta^{n-1}(N_{m-n} - \omega) + \omega - P_{m-1}\|^2 \quad (1)$$

Taking the first derivative with respect to N_0 and equating to zero, we have:

$$2(N_0 - P_0) + 2R_\theta^t(R_\theta(N_0 - \omega) + \omega - P_1) + ... + 2(R_\theta^{n-1})^t(R_\theta^{n-1}(N_0 - \omega) + \omega - P_{n-1}) = 0$$

or

$$nN_0 - n\omega + (\omega + R_\theta^t\omega + ... + (R_\theta^{n-1})^t\omega) - (P_0 + R_\theta^tP_1 + ... + (R_\theta^{n-1})^tP_{n-1}) = 0$$

Having the third term equal to the zero vector and noting that $R_\theta^t = R_{-\theta}$, we have:

$$N_0 = \frac{P_0 + R_{-\theta}P_1 + R_{-\theta}^2P_2 + ... + R_{-\theta}^{n-1}P_{n-1}}{n} + \omega$$

Similarly for each N_{in}, $i = 0 ... q - 1$, we obtain:

$$N_{in} = \frac{P_{in} + R_{-\theta}P_{in+1} + R_{-\theta}^2P_{in+2} + ... + R_{-\theta}^{n-1}P_{in+(n-1)}}{n} + \omega \quad (2)$$

Substituting (2) into (1), taking the derivative with respect to ω, and equating to zero we obtain:

$$m\omega = (P_0 + ... + P_{n-1}) + ... + (P_{m-n} + ... + P_{m-1}) + \frac{P_0 + R_\theta P_0 + ... + R_\theta^{n-1}P_0}{n} + ... + \frac{P_{m-n} + R_\theta P_{m-n} + ... + R_\theta^{n-1}P_{m-n}}{n}$$

or

$$\omega = \frac{P_0 + ... + P_{m-1}}{m}$$

Thus we showed that the center of mass is invariant under the symmetry transformation. Denoting $\tilde{P}_j = P_j - \omega$ and $\tilde{N}_j = N_j - \omega$ for all j, we obtain from (2) for each N_{in} ($i = 0...q-1$):

$$\tilde{N}_{in} = \frac{\tilde{P}_{in} + R_{-\theta}\tilde{P}_{in+1} + R_{-\theta}^2\tilde{P}_{in+2} + ... + R_{-\theta}^{n-1}\tilde{P}_{in+(n-1)}}{n}$$

i.e., when considering the center of mass as origin, we find that the transformed vector N_{in} equals the average of the vectors of the ith subgroup rotated toward P_{in} by $2\pi i/n$ radians.

Note that when $P_{in}, ..., P_{in+(n-1)}$ are C_n-symmetric about the center of mass, $\tilde{N}_{in} = \tilde{P}_{in}$ as expected.

Toward a Geometric Intuition. Assuming the center of mass ω is at the origin, denote by $\bar{P}_i$ the center of mass of the ith symmetry association $\{P_{in}, ..., P_{in+(n-1)}\}$. Let $\hat{P}_{in+j} = P_{in+j} - \bar{P}_i$ for $j = 0...n-1$ and $i = 0...q-1$. Substituting into (2) (with $\omega = 0$):

$$N_{in} = \frac{(\hat{P}_{in} + \bar{P}_i) + R_{-\theta}(\hat{P}_{in+1} + \bar{P}_i) + ... + R_{-\theta}^{n-1}(\hat{P}_{in+(n-1)} + \bar{P}_i)}{n}$$

and we have:

$$N_{in} = \frac{\hat{P}_{in} + R_{-\theta}\hat{P}_{in+1} + ... + R_{-\theta}^{n-1}\hat{P}_{in+(n-1)}}{n}$$

Thus we proved the optimality of the geometrical intuition of the symmetry transformation given in Section 3.2 and Section 3.3; i.e., apply the symmetry transform on each subgroup of vectors around their center of mass and then translate to the center of mass ω of all vectors (see Figure 7).

A.2. Reflection Symmetry. Given a set of vectors (whose source is the origin and destinations are points of an object) $P_0, ..., P_{m-1}$, we assume $m = 2q$. For simplicity we assume that the division into q pairs of vertices (as described in Section 3.4) is such that every two consecutive vectors constitute a pair (i.e., $\{P_{2i}, P_{2i+1}\}$ for $i = 0...q-1$). We wish to find the reflective-symmetry transformation of these vectors.

As in the C_n-symmetry case, we denote by $N_0, ..., N_{m-1}$ the vectors obtained from $P_0, ..., P_{m-1}$ under the symmetry transformation. Following the symmetry transformation definition, the following must be minimized over $N_0, ..., N_{m-1}$:

$$\|N_0 - P_0\|^2 + ... + \|N_{m-1} - P_{m-1}\|^2 \quad (3)$$

Following the definition of reflection symmetry, we have:

$$N_{2i+1} = R_{-\theta}R_fR_\theta(N_{2i} - \omega) + \omega \quad (4)$$

where ω is center of mass the transformed vectors, R_θ is a rotation matrix of angle θ about the origin, and R_f is a reflection matrix about the y axis. (i.e., for each pair, one transformed vector is a reflection of the other transformed vector about a line passing through the center of mass at angle θ to the y axis).

For clarity, we will set $R = R_{-\theta}R_fR_\theta$. Note that $R^t = R$ and $R^tR = I$. Substituting (4) into (3) we minimize:

$$\|N_0 - P_0\|^2 + \|R(N_0 - \omega) + \omega - P_1\|^2 + ... + \|N_{m-2} - P_{m-2}\|^2 + \|R(N_{m-2} - \omega) + \omega - P_{m-1}\|^2 \quad (5)$$

Taking the first derivative with respect to N_0 and equating to zero:

$$2(N_0 - P_0) + 2R^t(R(N_0 - \omega) + \omega - P_1) = 0$$

and

$$N_0 = \frac{P_0 + RP_1}{2} + \frac{\omega - R\omega}{2}$$

Similarly for each N_{2i}, $i = 0...q-1$

$$N_{2i} = \frac{P_{2i} + RP_{2i+1}}{2} + \frac{\omega - R\omega}{2} \quad (6)$$

Substituting into (5), taking the derivative with respect to ω, and equating to zero, we obtain:

$$2(I - R^t)(RP_1 - P_0 + (I - R)\omega) + ... + 2(I - R^t)(RP_{m-2} - P_{m-1} + (I - R)\omega) = 0$$

and

$$\omega = \frac{P_0 + ... + P_{m-1}}{m}$$

Thus, similar to the symmetry transformation for C_n symmetry, the center of mass remains invariant.

Without loss of generality we will assume the origin is at the center of mass. From (5) and (6) we must minimize:

$$\left\|\frac{RP_1 - P_0}{2}\right\|^2 + ... + \left\|\frac{RP_{m-1} - P_{m-2}}{2}\right\|^2 \quad (7)$$

Expanding $P_i = (X_i, Y_i)$, $i = 0...m-1$ and:

$R = R_{-\theta}R_fR_\theta =$

$$\begin{pmatrix} \cos\theta & -\sin\theta \\ \sin\theta & \cos\theta \end{pmatrix}\begin{pmatrix} -1 & 0 \\ 0 & 1 \end{pmatrix}\begin{pmatrix} \cos\theta & \sin\theta \\ -\sin\theta & \cos\theta \end{pmatrix} = \begin{pmatrix} -\cos 2\theta & -\sin 2\theta \\ -\sin 2\theta & \cos 2\theta \end{pmatrix}$$

Taking the derivative with respect to θ and equating to zero, we obtain:

$$\tan 2\theta = \frac{(X_0Y_1 + Y_0X_1) + ... + (X_{m-2}Y_{m-1} + Y_{m-2}X_{m-1})}{(X_0X_1 - Y_0Y_1) + ... + (X_{m-2}X_{m-1} - Y_{m-2}Y_{m-1})} \quad (8)$$

i.e., the reflection axis at angle θ (from the y axis) which satisfies (8), minimizes the symmetry distance of the object; thus the symmetry transformation transforms the object into a reflection-symmetric object with this reflection axis.

Note that two possible solutions exist for (8). It is easily seen that the solution which is the minimum is achieved when $\sin\theta\cos\theta$ is of opposite sign to the numerator of (8). Thus all N_i, $i = 0...m-1$, can be calculated and the symmetry transformation of $P_0, ..., P_{m-1}$ evaluated.

B. Extreme Cases: $S(C_n) = 100$. Following the CSM method the S values obtained are limited to the range 0...100. The lower bound of this range is obvious from the fact that the average of the square of the distances moved by the object points is necessarily positive. The upper bound of the average is limited to 1 since the object is previously normalized to maximum distance of 1, and by translation of all vertex points to the center of mass, a symmetric shape is obtained. (The average is thus less than or equal to 1 and the S value no more than 100.)

The value of $S(C_n) = 100$ is actually obtained for extreme cases such as a polygon of m vertices ($m = qn$) whose contour outlines a regular q-gon (i.e., every qth vertex of the m-gon coincides with a vertex of a regular q-gon). Thus an extreme case of C_2 symmetry is obtained for a polygon of six vertices whose contour describes a regular triangle (requiring a spiral of two cycles from P_0 to P_5); i.e., every pair of vertices of the 6-gon which are 3 apart along the contour, coincide with a vertex of the triangle (see Figure 18). The symmetry measure of this polygon is $S(C_2) = 100$, and its "closest" C_2-symmetric object is a point. This can easily be seen from the geometric description given in Section 3.3 and follows from the fact that, for each subset of two vertices, the folded and averaged vector (denoted $\tilde{P}_0$) coincides with the center of mass of the subset. Thus the C_2 symmetry of each pair is a point located at the centroid of the triangle, and we obtain the "closest" C_2-symmetric shape, a point located at the center of mass of the polygon. Thus, since the polygon is scaled initially, the average squared distance from vertex to center of mass is one.

C. Symmetry Transform in 3D: Computations. C.1. Rotational Symmetry. Given a set of vectors in 3D, $P_0, ..., P_{m-1}$, we assume $m = nq$. For simplicity we assume that the division into q subgroups of n vertices is such that every n consecutive vectors constitute a subgroup (i.e., $\{P_{in}, ..., P_{in+(n-1)}\}$ for $i = 0...q-1$ is a subgroup). We wish to find the C_n-symmetry transformation of these vectors.

Denote by $N_0, ..., N_{m-1}$ the vectors obtained from $P_0, ..., P_{m-1}$ under the symmetry transformation. Following the symmetry transformation definition, the following must be minimized over $N_0, ..., N_{m-1}$:

$$\|N_0 - P_0\|^2 + ... + \|N_{m-1} - P_{m-1}\|^2 \quad (9)$$

Without loss of generality, we assume the origin is at the center of mass (proof is similar to the 2D case given in Appendix A.1).

Following the definition of C_n symmetry in 3D, we have for each subgroup $i = 0...q-1$:

$$N_{in+1} = R_{\hat{n},-\theta}N_{in}$$

$$\vdots$$

$$N_{in+(n-1)} = R^{n-1}_{\hat{n},-\theta}N_{in}$$

where $R_{\hat{n},\theta}$ is the rotation by angle $\theta = 2\pi/n$ about the unit vector $\hat{n}$; i.e., for each subgroup, the transformed vectors form a regular n-gon on a plane perpendicular to the rotational axis with center of mass on the rotational axis.

Substituting in (9), taking the first derivative with respect to N_i and equating to zero, we have as in 2D for $i = 0...q-1$:

$$N_{in} = \frac{P_{in} + R_{\hat{n},\theta}P_{in+1} + R^2_{\hat{n},\theta}P_{in+2} + ... + R^{n-1}_{\hat{n},\theta}P_{in+(n-1)}}{n} \quad (10)$$

From (9) and (10) we must minimize the following over all possible rotational axes $\hat{n}$:

$$\|-(n-1)P_0 + R_{\hat{n},\theta}P_1 + ... + R^{n-1}_{\hat{n},\theta}P_{n-1}\|^2 + ... + \|R_{\hat{n},\theta}P_0 + ... + R^{n-1}_{\hat{n},\theta}P_{n-2} - (n-1)P_{n-1}\|^2 + ... \quad (11)$$

Using the Rodrigues formula, the first term of (11) becomes:

$$\| -(n-1)P_0$$
$$+(1-\cos(\theta))(\hat{n}\cdot P_1)\hat{n} \quad +\cos(\theta)P_1 \quad +\sin(\theta)(\hat{n}\times P_1)$$
$$+(1-\cos(2\theta))(\hat{n}\cdot P_2)\hat{n} \quad +\cos(2\theta)P_2 \quad +\sin(2\theta)(\hat{n}\times P_2)$$
$$\vdots \qquad \vdots \qquad \vdots$$
$$+(1-\cos((n-1)\theta))(\hat{n}\cdot P_{n-1})\hat{n}+\cos(n-1)\theta)P_{n-1}+\sin(n-1)\theta)(\hat{n}\times P_{n-1})\|^2$$

Denoting the vectors:

$$A_0 = -(n-1)P_0 + \cos(\theta)P_1 + \ldots + \cos((n-1)\theta)P_{n-1}$$
$$B_0 = (1-\cos(\theta))P_1 + \ldots + (1-\cos((n-1)\theta))P_{n-1}$$
$$C_0 = \sin(\theta)P_1 + \ldots + \sin((n-1)\theta)P_{n-1}$$

we obtain for the first term in (11);

$$\|A_0 + (\hat{n}\cdot B_0)\hat{n} + \hat{n}\times C_0\|^2$$

With similar expressions for all other terms, (11) can be written:

$$\sum_{j=0}^{m}\|A_j + (\hat{n}\cdot B_j)\hat{n} + \hat{n}\times C_j\|^2 \qquad (12)$$

We minimize (12) over all possible vectors n under the constraint $\|n\| = 1$. Using Lagrange multipliers we obtain the following nonlinear system of matrix equations:

$$Mn + H - \lambda n = 0$$
$$n^t n - 1 = 0$$

where M is the matrix: $\sum_{j=0}^{m}(B_jB_j^t + C_jC_j^t + A_jB_j^t + B_jA_j^t)$, H is the vector $\sum_{j=0}^{m}(C_j \times A_j)$, and λ is the Lagrange multiplier.

Several numerical methods are available for solving such nonlinear systems. We used a variant of the iterative Newton method. This method requires initial values which we chose as the principal axes of the object whose C_n symmetry we are measuring (iteratively solving the system for each principal axis and choosing the best solution).

C.2. Reflection-Symmetry. Given a set of vectors in 3D, P_0, ..., P_{m-1}, we assume $m = 2q$. For simplicity we assume that the division into q pairs of vertices (as described in Section 3.4) is such that every two consecutive vectors constitute a pair (i.e., $\{P_{2i}, P_{2i+1}\}$ for $i = 0...q-1$). We wish to find the reflective-symmetry transformation of these vectors. Given a reflection plane, $S(\sigma)$ is calculated (according to eq 7 and similar to the description given in Section 3.4 for the 2D case) by reflecting one vector from each pair across the reflection plane, averaging with the other vector of the pair, and reflecting back the obtained average vector (see also Figure 8). In the general case, where the reflection plane is not known a priori, a minimization process must be adopted to find the reflection plane that minimizes the symmetry distance. We chose a gradient descent method which incrementally changes the reflection plane so that the CSM value is decreased at each iteration. The process converges to the reflection plane minimizing the symmetry distance.

A New Look at an Old Ligand: Surprises with Thioethers. A Density Functional Study

Heiko Jacobsen, Heinz-Bernhard Kraatz, Tom Ziegler,* and P. Michael Boorman

Contribution from the Department of Chemistry, University of Calgary, 2500 University Drive N.W., Calgary, Alberta, Canada T2N 1N4. *Received December 10, 1991*

Abstract: Using approximate density functional theory (DFT), the electronic and geometrical structures of thioether-containing d^3–d^3 face-sharing bioctahedral complexes of the type $[Mo_2Cl_{9-n}(SH_2)_n]^{n-3}$, with n = 2, 3, 4, 5, and $(SH_2)Cl_2Mo(\mu\text{-}Cl)_2(\mu\text{-}SR_2)MoCl_2(SH_2)$, with R = H, F, CH_3, are studied. All structures have been partially optimized and are in good agreement with the experiment. The fact that a thioether possesses one lone pair less than chloride decreases the repulsive interaction within the bridge. This and the availability of an empty σ^* orbital on the thioether ligand are largely responsible for a remarkable shortening of the Mo–Mo bond. All $(\mu\text{-}Cl)_3$ complexes exhibit a high-spin configuration with a long Mo–Mo distance (282 pm–268 pm), whereas the systems with one or more SR_2 ligands in the bridge has a low-spin configuration with a short Mo–Mo bond (256 pm–246 pm). The spin-coupling constant J_{ab}[Ia] of the antiferromagnetic complex $[(SH_2)Cl_2Mo(\mu\text{-}Cl)_3MoCl_2(SH_2)]^-$ (Ia) has been calculated to be -385 cm^{-1}, in close agreement with experimental coupling constant for related systems. Fragment analysis shows that the largest contribution to bonding clearly stems from σ donation of electron density from the sulfur's lone pairs (p_x and sp-hybrid). The σ-donor strength increases as follows: $S(CH_3)_2 > SH_2 > SF_2$. However, back-donation from the metal centers to a vacant σ^* orbital of the bridging thioether represents a sizable portion of the overall bonding energy. Expectedly, the π-acceptor ability of thioethers increases upon an increased electronegativity of the substituent on the thioether. Back-bonding is of lesser importance for terminal thioethers.

1. Introduction

A proper description of unsupported metal–metal bonds in naked dimers as well as binuclear complexes has been one of the more intriguing challenges to modern computational chemistry concerned with electronic structure theory. Intense scrutiny has been given to the hextuple bonded M_2 (M = Cr, Mo, W) dimers[1-5] as well as the quadruple[3,6-10] and triple bonded[11] binuclear complexes of the chromium triad. Many of the difficulties originate from the presence of σ- as well as π- and δ-bonds with vastly different requirements in terms of electron correlation. The computational problems are compounded further by the need to give a proper description of the relative involvement from the rather diffuse s-type orbitals as well as the more contracted d orbitals. It is still far from routine to provide a quantitative

(1) Delley, B.; Freeman, A. J.; Ellis, D. E. *Phys. Rev. Lett.* **1983**, *50*, 488.
(2) Baycara, N. A.; McMaster, B. N.; Salahub, D. R. *Mol. Phys.* **1984**, *52*, 891.
(3) Ziegler, T.; Tschinke, V.; Becke, A. *Polyhedron* **1987**, *6*, 685.
(4) Goodgame, M. M.; Goddard, W. A., III *Phys. Rev. Lett.* **1985**, *54*, 661.
(5) Bursten, B. E.; Cotton, F. A.; Hall, M. B. *J. Am. Chem. Soc.* **1980**, *102*, 6348.
(6) Ziegler, T. *J. Am. Chem. Soc.* **1984**, *106*, 5901.
(7) Ziegler, T. *J. Am. Chem. Soc.* **1985**, *107*, 4453.
(8) Benard, M.; Wiest, R. *Chem. Phys. Lett.* **1985**, *122*, 447.
(9) Hall, M. B. *Polyhedron* **1987**, *6*, 679.
(10) Bursten, B. E.; Clark, D. L. *Polyhedron* **1987**, *6*, 695.
(11) Ziegler, T. *J. Am. Chem. Soc.* **1983**, *105*, 7543.

0002-7863/92/1514-7851$03.00/0 © 1992 American Chemical Society